A NEURAL NETWORK APPROACH TO RETRIEVE SINGLE SCATTERING ALBEDOS AND TEMPERATURES FROM THEMIS AND TES INFRARED DATA OVER GALE CRATER.

T. Condus[1], R. E. Arvidson[1], L. He[2], J. A. O'Sullivan[2], M. J. Wolff[3], and R. V. Morris[4], [1]Dept. of Earth and Planetary Sciences, Washington University in St. Louis, St. Louis, MO (tcondus@wustl.edu), [2]Preston M. Green Dept. of Electrical and Systems Engineering, Washington University in St. Louis, St. Louis, MO, [3]Space Science Institute, Boulder, CO, [4]NASA Johnson Space Center, Houston, TX.

Introduction: The Mars Odyssey Thermal Emission Imaging System (THEMIS) [1] and the Mars Global Surveyor Thermal Emission Spectrometer (TES) [2] have mapped the Martian surface in the thermal infrared (~6.8 to 14.9 µm and ~6 to 50 µm, respectively), providing a large archive of data for thermophysical and mineralogic studies with global-scale coverage. The thermal infrared wavelength region is complementary to VNIR for studying mineralogy, because it is where the stretching and bending fundamental vibrational modes for classes of minerals such as silicates, sulfates, and carbonates occur.

Thermal emittance is highly dependent on surface kinetic temperature – without knowing this, retrieval of single scattering albedos (SSA) or directional emissivity from emittance measurements is an underdetermined and ill-posed problem. We have modified the neural network methodology called STANN (Separating Temperature and Albedo by Neural Networks) developed by [3] to separate the effects of surface kinetic temperature from THEMIS and TES spectral emittance data in order to solve for SSA spectra and surface kinetic temperatures at every pixel in a given scene.

Data Modeling: We use DISORT [4] to model spectral emittance on sensor, on a per-scene basis. The Hapke bidirectional reflectance function [5] is provided as the surface boundary condition, which is integrated over all viewing angles and complemented using Kirchhoff's Law to obtain a directional-hemispherical form for emittance for each wavelength. Scene-appropriate surface kinetic temperatures, and a likely range of SSA values serve as inputs, while accounting for the effects of dust and ice aerosols and atmospheric CO_2 and water vapor. A multi-dimensional lookup table is created, with the DISORT input parameters on the axes, and the spectral emittances as the entries. As long as the spectral emittance on sensor and surface kinetic temperature are known for a given pixel in a scene, then a series of interpolations through the table can be performed to find the corresponding SSA value (see Figure 1 for example DISORT-modeled spectra).

Neural Network: For THEMIS and TES, STANN uses a design that is similar to what was used for CRISM [6] data at wavelengths > ~2.7 µm [3, 7]. THEMIS has 7 usable bands from 7.93 to 12.57 µm. To account for the small amount of spectral information, the data are oversampled to ~50 bands and used as the STANN input. SSA spectra and a surface kinetic temperature for each pixel are the outputs. For TES, the number of bands used is 60 (from ~7 to 12 µm), i.e., a subset without bands dominated by atmospheric CO_2 and water vapor absorptions. We use a single hidden layer, with the heuristic that the number of nodes is the same as the number of input bands. For each hidden layer node, a rectifier is used as the activation function. These rectifiers, combined with the weights of edges between layers, are used to map inputs to outputs.

Initially, the weights on edges are unknown and at first are assigned arbitrary values. Therefore, the neural network must be trained so that the correct weights can be found. Since adjacent layers in the neural network are fully connected, there are ~5,000 unknown weights for THEMIS and ~10,000 unknown weights for TES. A number of training examples that is ~10 times the amount of weights are generated. Linear combinations of laboratory reflectance spectra of likely Mars minerals and rocks are created, in order to simulate THEMIS or TES SSA emittance spectra. Each training example consists of a simulated SSA spectrum combined with a randomly selected value of surface kinetic temperature appropriate for a given scene, along with its corresponding spectral emittance spectrum retrieved by using the DISORT lookup table. During training, estimates of SSA and surface kinetic temperature are produced based on the current weights in the neural network. The root-mean-square error (RMSE) between the estimates and the real values provided in the training examples are calculated and then backpropagated to the hidden layer. A gradient descent algorithm uses this information to update the weights and the process is repeated across all training examples until the RMSE is small enough.

After the training phase, the neural network is given actual THEMIS or TES spectral emittance data. The retrieved temperature map is used to solve for SSA at every pixel, after resampling to 7 bands for THEMIS.

Results: STANN was applied to THEMIS scene I54337024 and TES orbit 19233, which were taken during winter over Mount Sharp in Gale Crater (Figure 2). Scene I54337024 was acquired while Curiosity was present, and the STANN-derived surface kinetic temperature for that location was 221 K. At the same local true solar time of 17.47, the REMS radiometer on Curiosity [8] measured an interpolated surface kinetic temperature of 222 K. The THEMIS brightness temperature of the same pixel is 217 K. For TES orbit 19233 data, the STANN-derived surface kinetic temperatures and TES estimated temperatures for different geologic units are shown in Figure 2. In general, the THEMIS brightness temperatures and TES estimated temperatures are lower than the STANN-derived surface kinetic temperatures due to the loss of photons traveling from ground to sensor (i.e., they are calculated from radiance data without atmospheric correction).

Example TES spectra for different geologic units within Gale Crater are shown in Figure 3. The sulfate-bearing unit exhibits an ~8.5 µm Reststrahlen feature consistent with sulfate mineral fundamental stretching vibration [9]. The dune field has a Reststrahlen feature consistent with the presence of olivine. The crater floor and upper dust stone unit have an SSA high (or emissivity low) at around 7.1 µm, which is associated with high dust cover [10]. Overall, our STANN-retrieved TES emissivity spectra are similar in shape to the emissivity spectra retrieved according to the methods of [11].

Future Work: We plan to apply STANN to a synthesis of CRISM, OMEGA [12], THEMIS, and TES scenes over Gale Crater for a similar solar longitude, and retrieve SSA spectra covering the wavelength range from ~0.4 to 25 µm. Our goal is to be able to invert the SSA spectra using a combination of Hapke modeling [5] and singular value decomposition to retrieve information about mineral abundances, grain sizes, and packing, e.g., within the sulfate-bearing strata. We are continuing to explore DISORT parameter space and neural network options to better constrain SSA values. Finally, we are pursuing an effective way to model the atmospheric water absorptions centered at ~6 µm to be able to extract the carbonate fundamental stretching Reststrahlen absorption, which would be useful for studying mineralogy in areas such as Jezero Crater [13].

References: [1] Christensen P. R. et al. (2004) *Space Sci. Rev., 110*(1-2), 85-130. [2] Christensen P. R. et al. (2001) *JGR: Planets, 106*(E10), 23823-23871. [3] He L. et al. (2019) *LPS L*, these abstracts. [4] Stamnes K. et al. (1988) *Appl. Opt., 27*, 2502-2509. [5] Hapke B. (1993) *Theory of Reflectance and Emittance Spectroscopy*. [6] Murchie S. et al. (2007) *JGR: Planets, 112*(E5). [7] Powell K. E. et al. (2017) *LPS XLIX*, Abstract #2113. [8] Gómez-Elvira J. et al. (2012) *Space Sci. Rev., 170*(1-4), 583-640. [9] Cloutis E. A. et al. (2006) *Icarus, 184*(1), 121-157. [10] Ruff S. W. and Christensen P. R. (2002) *JGR: Planets, 107*(E12), 2-1. [11] Smith M. D. et al. (2000) *JGR: Planets, 105*(E4), 9589-9607. [12] Bibring J. P. et al., (2005) *Science*. [13] Ehlmann B. L. et al. (2008) *Science, 322*(5909), 1828-1832.

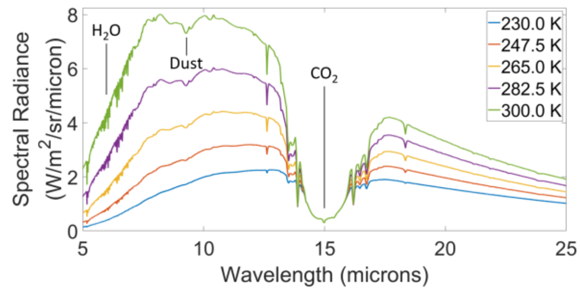

Figure 1. Plot of DISORT-modeled spectral emittance spectra for a range of temperatures, with an emergence angle of 0.55° and an SSA of 0.17. Absorptions due to atmospheric gases and aerosols are shown.

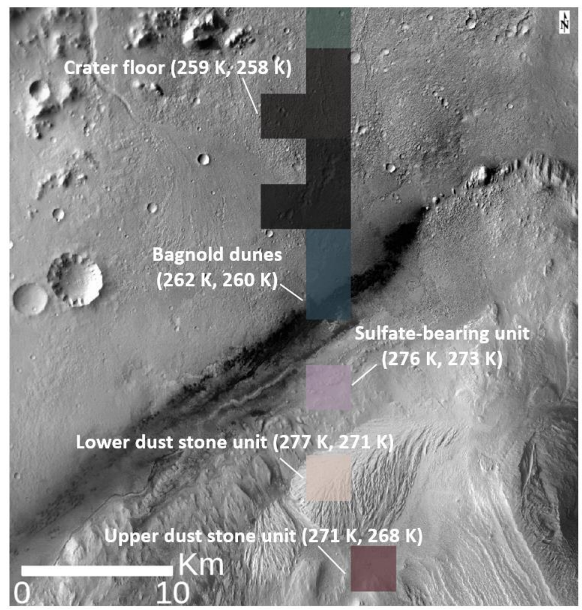

Figure 2. TES orbit 19233 SSA map overlain on THEMIS VIS mosaic of lower Mount Sharp in Gale Crater. Distinct geologic units are labeled with STANN-retrieved temperatures followed by TES estimated temperatures. RGB: (8.48 µm, 8.88 µm, 9.32 µm).

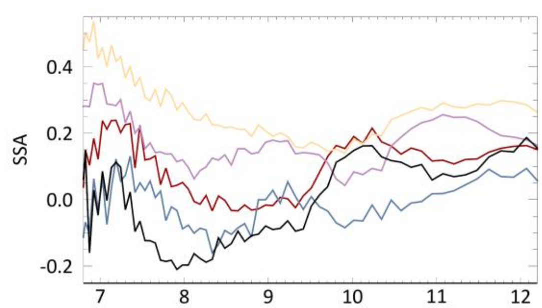

Figure 3. TES STANN-retrieved SSA spectra for different geologic units within Gale Crater. Spectra colors correspond to colors of labeled TES pixels in Figure 2.